minerals

MDPI

Article

Mineralogical Characterization of Dolomitic Aggregate Concrete: The Camarasa Dam (Catalonia, Spain)

Encarnación Garcia [1], Pura Alfonso [2,*] and Esperança Tauler [3]

[1] Departament d'Enginyeria Electrònica, Escola d'Enginyeria de Barcelona Est (EEBE), Universitat Politècnica de Catalunya Barcelona Tech, Av. d'Eduard Maristany 16, E-08019 Barcelona, Spain; encarna.garcia.vilchez@upc.edu

[2] Departament d'Enginyeria Minera, Industrial i TIC, Universitat Politècnica de Catalunya Barcelona Tech, Av. Bases de Manresa 61-63, 08242 Manresa, Barcelona, Spain

[3] Departament de Mineralogia, Petrologia i Geologia Aplicada, Universitat de Barcelona, Carrer Martí i Franquès s/n, 08028 Barcelona, Spain; esperancatauler@ub.edu

* Correspondence: maria.pura.alfonso@upc.edu; Tel.: +34938777292

Received: 31 December 2019; Accepted: 26 January 2020; Published: 29 January 2020

Abstract: The Camarasa Dam was built in 1920 using dolomitic aggregate and Portland cement with two different compositions: type A (dolomite and Portland cement) and type B (dolomite and sand-cement). The sand cement was a finely powdered mixture of dolomite particles and clinker of Portland cement. The mineralogy of concrete was studied by optical microscopy, scanning electron microscopy, and x-ray powder diffraction. Reaction of dedolomitization occurred in the two types of concrete of the Camarasa Dam, as demonstrated by the occurrence of calcite, brucite, and/or absence of portlandite. In the type A concrete, calcite, brucite, and a serpentine-group mineral precipitated as a rim around the dolomite grains and in the paste. The rims, a product of the dedolomitization reaction, protected the surface of dolomite from the dissolution process. In type B concrete, in addition to dolomite and calcite, quartz and K-feldspar were present. Brucite occurred in lower amounts than in the type A concrete as fibrous crystals randomly distributed in the sand-cement paste. Although brucite content was higher in the type A concrete, type B showed more signs of loss of durability. This can be attributed to the further development of the alkali-silica reaction in this concrete type.

Keywords: dolomite; sand-cement; concrete; dedolomitization reaction

1. Introduction

Concrete made of dolomite aggregate, has been the source of problems such as expansion and cracking [1–7]. Traditionally, these deterioration problems were associated with the alkali-carbonate reaction (ACR) [8,9], which is produced when dolomitic rocks with clay minerals are used as aggregates or as a result of the reaction of dolomite with cryptocrystalline quartz [10]. Several dams, built with carbonate aggregates, exhibit signs of deterioration such as the Bimont Dam in France, constructed with dolomitic limestones [11], and the Chickamagua Powerhouse Dam in Tennessee [12].

Dolomite aggregate in the presence of hydrated Portland cement paste produces the dedolomitization Reaction (1):

$$\underset{\text{dolomite}}{CaMg(CO_3)_2} + \underset{\text{portlandite}}{Ca(OH)_2} \rightarrow 2\underset{\text{calcite}}{CaCO_3} + \underset{\text{brucite}}{Mg(OH)_2} \quad (1)$$

Dolomite reacts with the portlandite of the cement paste to produce calcite and brucite. The kinetics of this reaction have been studied in different alkaline media, temperatures, and silica content [13–16].

The occurrence of the ACR can be checked using a combination of different techniques. Petrographic study is a preliminary test to evaluate the reactive potential of the aggregates and to identify the location of the chemical reactions [17]. The morphological characteristics of the aggregate particles and their textures have an important role in the properties and durability of concrete [18–20]. The effective reactive surface area is a critical parameter to the kinetics and depends on the surface morphology, surface roughness, and internal structure (dislocation density, impurities, point defects) of the mineral representing highly localized dissolution [21]. For this, accelerated testing of mortar specimens is usually used to determine the reactive aggregates [22,23]. However, the study of dolomitic concrete from old constructions could be a real study case that contributes with data to understand this reaction.

At the beginning of the 20th century, several dams were built with a new agglomerate called sand-cement. Sand-cement was patented in Copenhagen in 1893, and consisted of 45 wt% of siliceous particles and 55 wt% of clinker of Portland cement, powdered up to less than 0.1 mm in size [24]. The concrete performed with this new product was largely investigated in the USA, where good mechanical properties were reported: impermeability, low drying shrinkage because of the short increase of temperature, and low setting time [25]. Other advantages of the sand-cement were that it was cheaper than the Portland cement and was obtained in the manufacturing plant of the dam. The new agglomerate was used to construct dams such as Arrowrock in 1915 and Elephant Butte in 1916, in the USA and Camarasa in 1920 and Tranco de Beas in 1934 in Spain.

The Camarasa water reservoir is used for water storage and the production of hydroelectric power. It is a 92 m high gravity dam. When it was constructed between 1917 and 1920 [26], it was the first in Europe and the fourth in the world in height. The Camarasa concrete was made with a binder material used for building several dams at that time named sand-cement. This was constituted by dolomitic fine particle aggregates.

In the present work, the petrography and mineralogical composition of concrete from the Camarasa Dam was studied, a hundred years after its construction, to assess the development of the ACR and thus, the concrete durability. The Camarasa Dam can be considered as a natural laboratory to study the reaction of dedolomitization in concrete. The characterization of this concrete can illustrate the behavior of an ancient hydraulic construction made of dolomitic aggregate and of sand-cement composed of a high fraction of very small particles of dolomite, which, in an alkaline media, are highly reactive.

2. Materials and Methods

2.1. Materials

The Camarasa Dam was constructed with Portland cement and dolostones in its vicinity. It is located on the Noguera-Pallaresa channel river, just before the confluence with the Segre River (Figure 1). This area is constituted of Jurassic carbonated rocks of the Mesozoic Tremp Basin in the marginal Sub-Pyrenean Zone (Spain). The dam is hosted in dolomitic rocks constituted by massive dark beds, with abundant dissolution cavities filled of calcite crystals, up to one cm in size [27]. The raw dolostones exhibit a sparitic texture with dolomite subhedral crystals of up to 1.0 mm in size. They are composed of almost pure dolomite, with less than 1 wt% of calcite (Figure 2). Calcite is not homogenously distributed; it constitutes interstitial cement or is located in the rims around the dolomite crystals; occasionally dolomite crystals are surrounded by calcite crystals formed by a dedolomitization process.

The raw rocks were crushed and selected according its grain size at the manufacturing plant located beside the dam, at a higher level to transport the materials by gravity. Several blocks of dolostones (15% of the total volume of concrete), were deposited in the basis and in the inner parts of the dam in order to increase the whole density and make the structure more stable [26].

According to the dose, two types of concrete, A and B, were used for the construction of the Camarasa Dam (Figure 1b). The basis of the dam was built with 32.559 m^3 of type A concrete, composed of 9 wt% of Portland cement and 91 wt% of dolomitic aggregate.

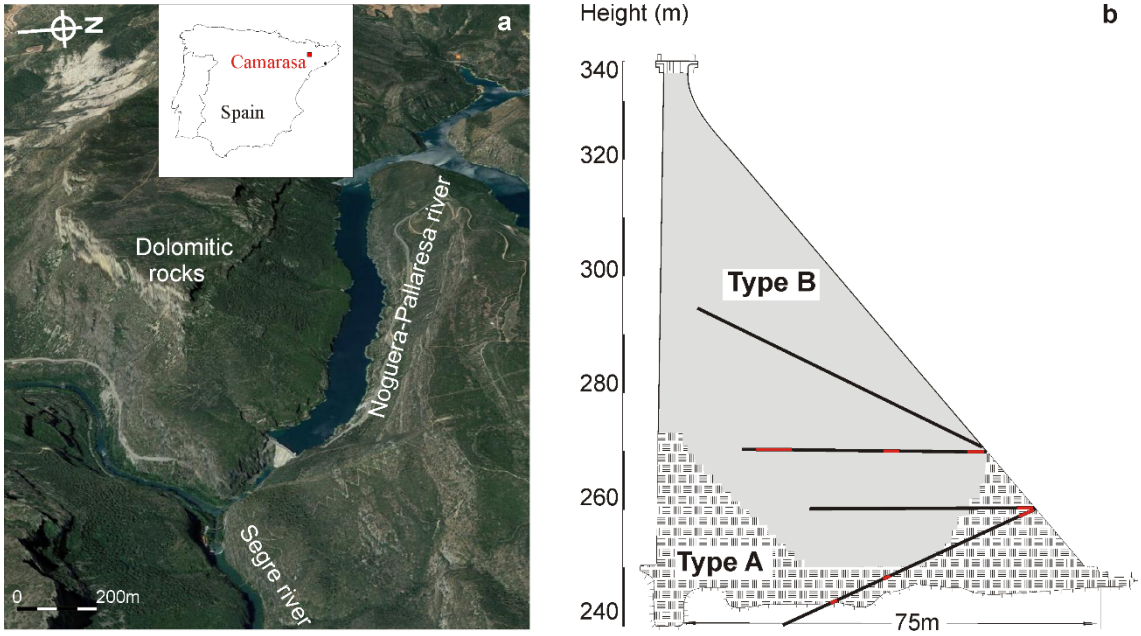

Figure 1. (**a**) View of the Camarasa Dam; (**b**), sketch with the distribution of the two concrete types (modified from [26] and the location of the cores (black lines) and samples (red)).

Later, in order to reduce the costs, the Portland cement was substituted by the sand-cement mixture, and 183.839 m^3 of type B concrete were used to finish building the dam [27]. The total composition of this concrete consisted of 5.2 wt% of Portland cement and 94.8 wt% of dolomite. The sand-cement used in this dam was a homogeneous mixture of 55 wt% of clinker of Portland cement and 45 wt% of dolomite pounded together up to less than 0.13 mm in size. The composition of the two concrete types is presented in Table 1.

The concrete was studied in ten drill cores of 55 mm in diameter, obtained in 1998 by the electric power company, owner of the dam.

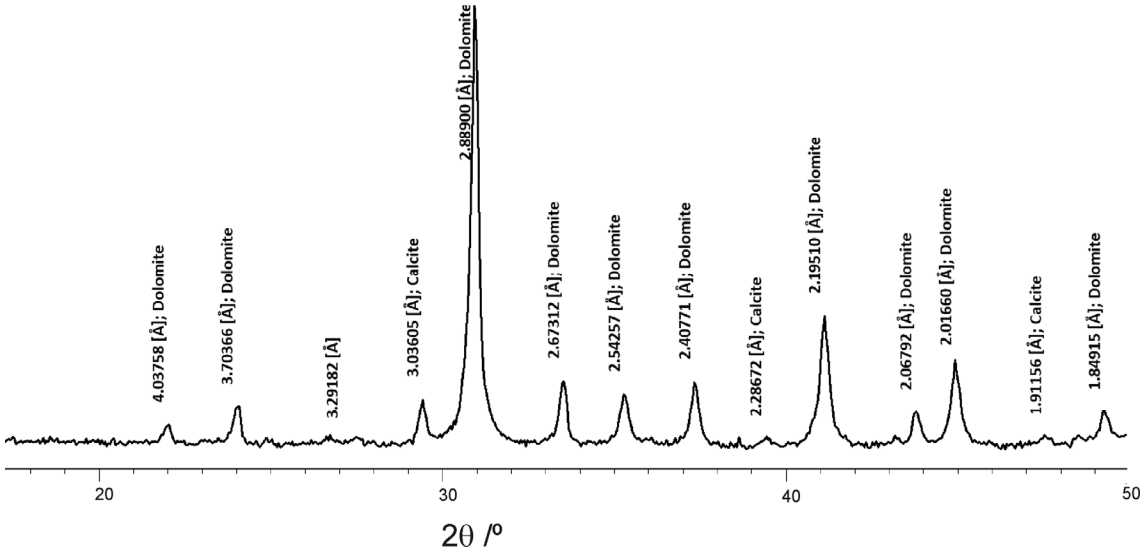

Figure 2. XRPD (X-ray powder diffraction) pattern of the dolostones used as aggregates to make the Camarasa concrete.

Table 1. Composition of type A and type B concrete [26].

Component	Particle Size (mm)	Type A (wt%)	Type B (wt%)
Dolomitic aggregate	10–150	-	66
Dolomitic aggregate	10–70	62	-
Dolomitic aggregate	1–10	13	12
Dolomitic aggregate	0.1–1	12.2	10.8
Dolomitic aggregate	<0.1	3.8	6
Portland cement		9.0	5.2

2.2. Analytical Methods

Thin sections were made from the cores with non-aqueous polishing fluids and epoxy resin adhesives to prevent the dissolution of mineral phases. Several thin sections were stained with Alizarin Red S+ Potassium to evaluate the composition of carbonate minerals.

Thin sections were studied by electronic microscopy with x-ray energy dispersive spectroscopy (SEM + EDS); images and qualitative analyses were produced using a Leika Stereoscan 360, an ESEM Quanta 200 FEI, XTE 325/D8395 and a field emission scanning electron microscope JEOL JSM-7001F at the Serveis Científics i Tecnològics de la Universitat de Barcelona (CCiTUB).

The x-ray powder diffraction (XRPD, Siemens AG, Munich, Germany) was used to determine the mineral phases present in the concrete. Measurements were performed in a Bragg-Brentano θ2θ Siemens D-500 diffractometer (radius = 215.5 mm) with Cu Kα radiation, selected by means of a secondary graphite monochromator. The divergence slit was 1° and the receiving slit of 0.15°. The step size was 0.05° 2θ and the measuring time was 10 seconds per step. For the calculation of the mineral phase contents, the quantitative Rietveld analysis method with the FULLPROF program [28] was used. The analyses were made at the CCiTUB.

3. Results

3.1. Raw Dolostones

The rocks used as aggregates were mainly constituted by dolomite up to 89 wt% and calcite up to 11 wt% (Figure 2). The occurrence of calcite is the result of the dedolomitization process of the raw dolostones before being exploited. Brucite was been observed in any case.

Under the microscope, the dolomite crystals exhibited a turbid appearance due to the content of abundant internal inclusions forming dark and clear bands, or a zebra texture (Figure 3). Calcite constituted the interstitial cement or was located in the rims around the dolomite crystals (Figure 3b) or in grains of dolomite in the natural process of dolomitization forming path textures.

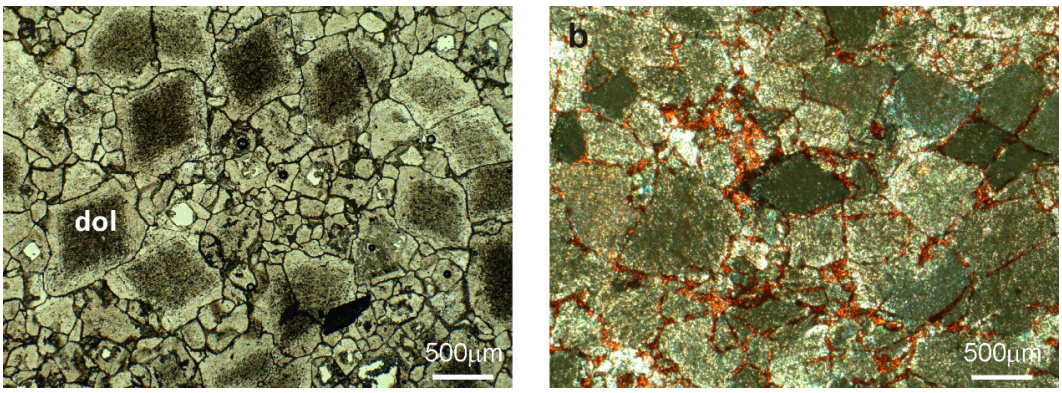

Figure 3. Textures of raw dolomitic rocks: (**a**) The most abundant dolomite aggregates with a zebra texture. (**b**) The dolomite rock dyed with a solution of Alizarin Red S + 0.9g showed natural dedolomitization; the red matrix is calcite.

3.2. Concrete Petrography and Mineralogy

Type A and type B concrete can be distinguished by the color of the cement paste: type A is light grey, whereas type B is dark brown (Figure 4). The visual inspection showed significant differences between the type A and type B concrete. Type A looked more compact and was more resistant to abrasion, whereas the type B concrete was more disagreeable. It was expected, then, that the behavior of the dedolomitization reaction would be considerably different in the two concrete types.

Figure 4. Fragments of cores from the Camarasa Dam. (**a**) Type A concrete; (**b**) type B concrete; (**c**) core section: the left half is made up of type B concrete and the right half is type A.

Aggregate particles from the Camarasa Dam exhibited an equant and angular shape, and did not look weathered. The most abundant aggregates were grey-brown particles constituted of pure dolomite grains.

Under the microscope, the type A and type B concrete showed a random distribution of the different particle size fractions of dolomitic particles (Figure 5a). Unconnected porosity was randomly distributed in the paste. The thin sections stained with red alizarin show red rims in the contact between the cement paste and the particles of the dolomitic aggregate (Figure 5b).

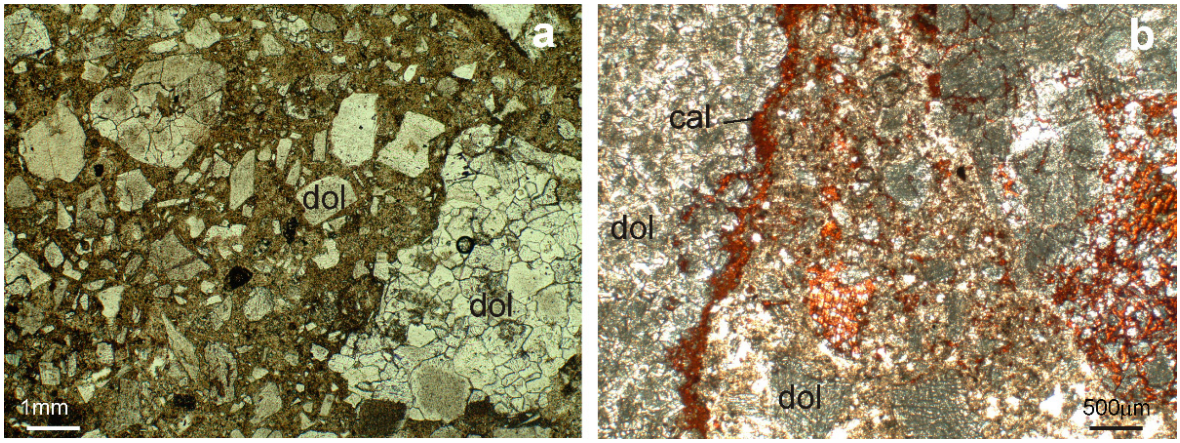

Figure 5. Microscope image of the Camarasa type A concrete. (**a**) General view; (**b**) sample stained with red alizarin that shows a red rim of calcite in the contact dolomite aggregate-paste. dol, dolomite; cal, calcite.

Dolomite and calcite are the major components in the paste of both concrete types. Other crystalline phases detected were different in them (Table 2). In order to evaluate the reactions produced in the Camarasa Dam aggregates, we describe the differences found in the chemical and mineralogical characteristics of the two concrete types.

Table 2. Mineralogical composition of the paste from type A (convectional) and type B concrete (with sand-cement).

Type	Sample	Calcite	Dolomite	Quartz	Brucite	Microcline
A	5bi-1	35	52	-	13	-
A	5bi-2	27	66	-	7	-
A	P5bc	56	40	2	2	-
B	4a	16	66	11	1	6
B	13a	18	59	15	1	7
B	P4a	18	67	11	<1	4
B	P6a	19	65	11	<1	4
B	P10a1	18	65	12	<1	5
B	P10a2	26	55	13	1	5

3.2.1. Type A Concrete

XRPD and SEM show that in the type A cement paste, in addition to dolomite and calcite, a significant amount of brucite and portlandite was also present (Figure 6).

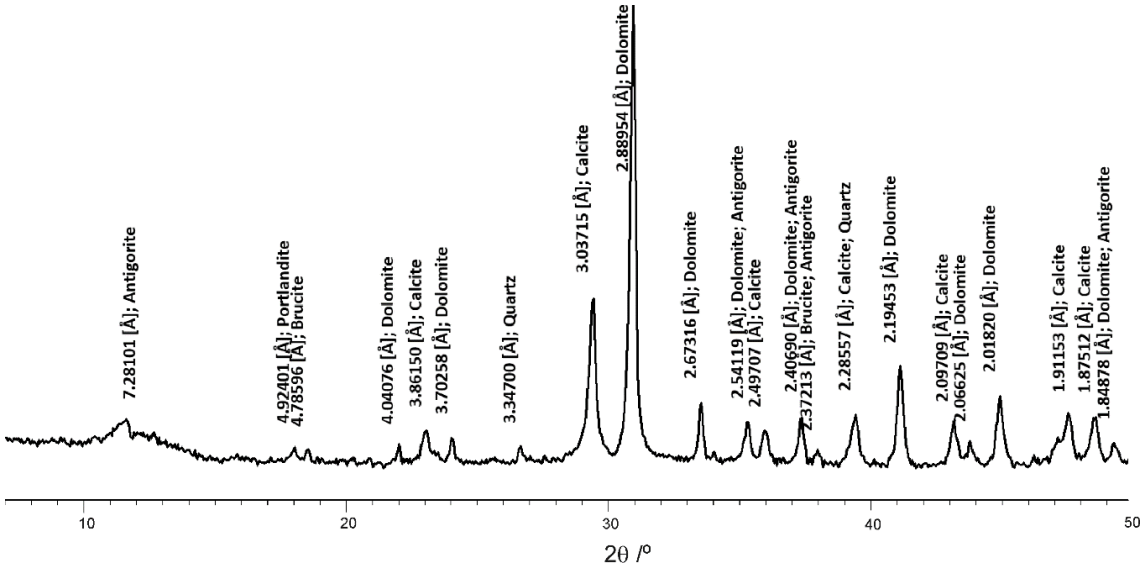

Figure 6. XRPD pattern of the cement paste of type A concrete.

EDS analyses of dolomite crystals reveal approximately 25 µm wide compositional rims (Figure 7). The chemical composition of mineral phases from these rims in the contact with the cement paste is Mg, Al, Si-rich and indicates that their mineralogy is constituted by brucite and a member of the serpentine group minerals (Figure 7).

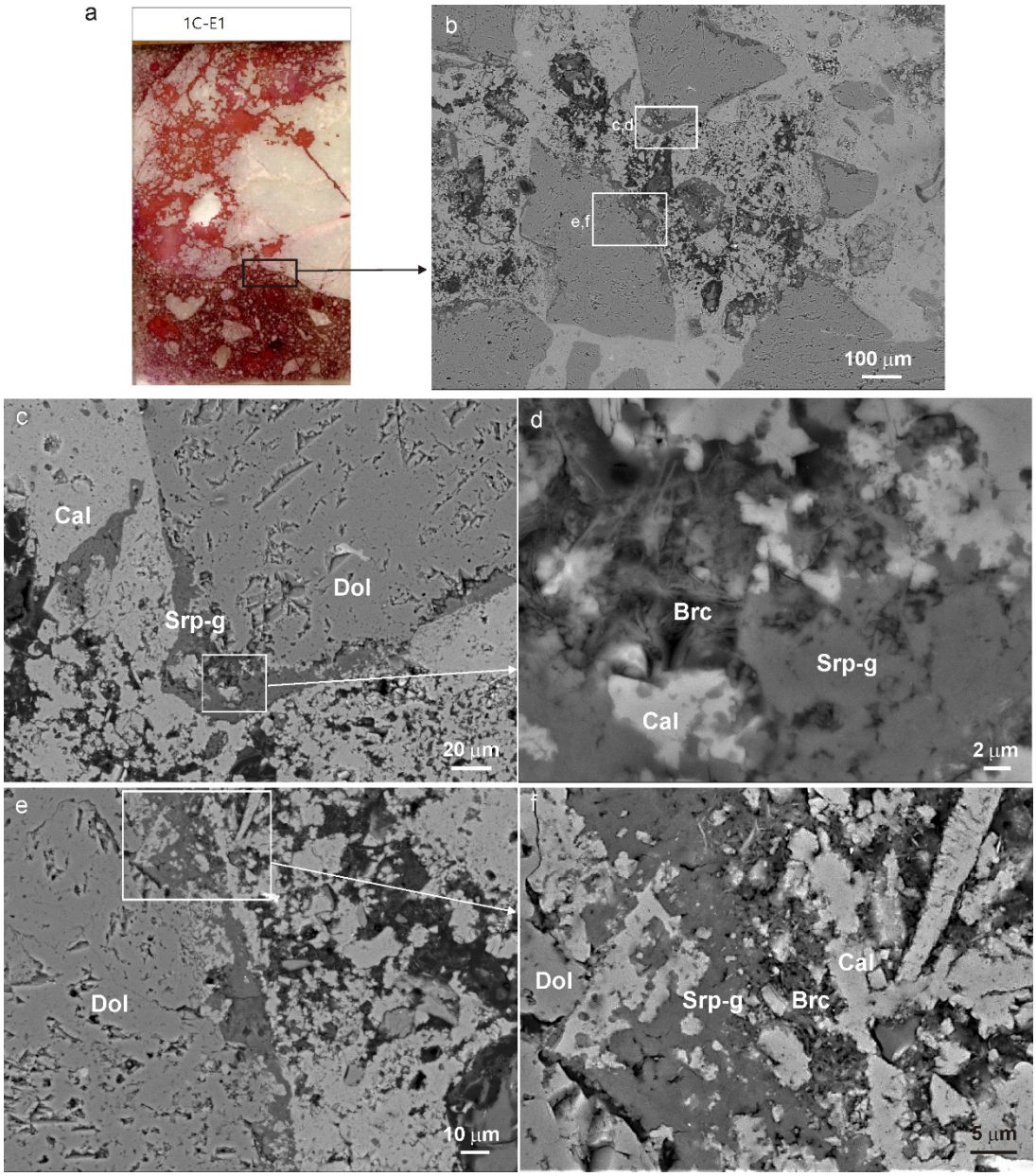

Figure 7. (**a**) Image of a thin section of type A concrete stained with red alizarin, where calcite is red stained and dolomite is not stained. (**b**) BSC-SEM Image of two selected zones with aggregate dolomite particles showing grey rims of reaction between aggregate particles and cement paste; (**c**) Zoom of the rim on top (**c,d**) with the mineral phases identified by SEM-EDS, dolomite (dol), calcite (Cal), serpentine group mineral (Srp-g); (**d**) zoom of the image c, brucite (Brc) is detected by SEM-EDS forming radial aggregates of fibrous crystals or elongated crystals maximum 6 μm; (**e,f**) Zoom of other rim of dolomite, where elongated brucite crystals appears in contact with a cryptocrystalline serpentine-group mineral and calcite crystals with irregular borders.

3.2.2. Type B Concrete

The XRPD of the paste in the type B concrete indicates that the crystalline phases were mainly dolomite, calcite, brucite, quartz, and K-feldspar. In this type of concrete, portlandite was not detected and the contents of brucite were significantly lower than in the type A concrete (Table 2). The presence of quartz and K-feldspar was probably due to the addition of sand from the channel river and from Cretaceous sandstones of the area during the manufacturing process of the sand-cement. The SEM

observations confirm the presence of brucite crystals up to 10 μm in size, with platelets or fibrous habit (Figure 8).

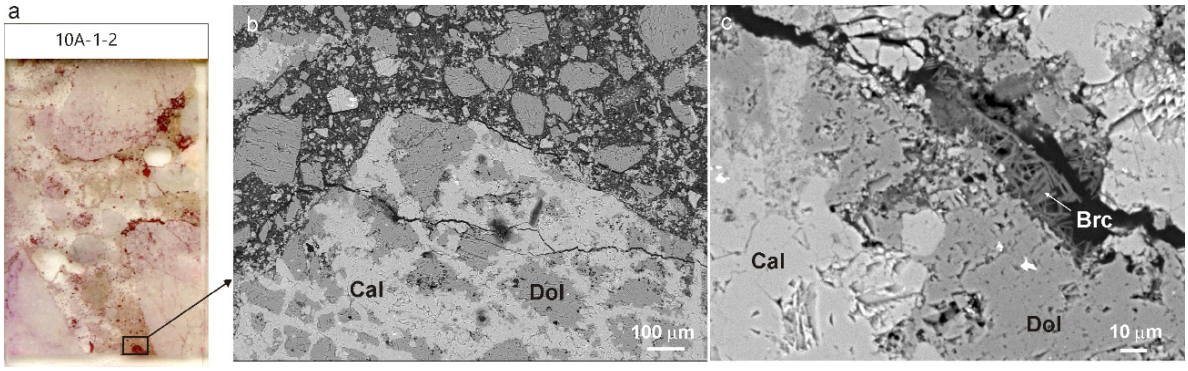

Figure 8. (**a**) Image of a thin section of type B concrete stained with red alizarin; (**b**,**c**) SEM images of the dolomite- and-cement paste contact in type B concrete with the development of fibrous brucite.

In addition, the SEM observations also showed the occurrence of ettringite and belite. Some illite elongated crystals were detected by SEM-EDS, and nests of belite, "bunch of grapes", with dark hydration rims dispersed in the interstitial component or paste could occasionally be observed (Figure 9a), indicating that the hydration of cement was not complete. Unconnected porosity was randomly distributed in the paste. Most cavities exhibited recrystallization rims or were totally or partially filled of calcite, ettringite, or portlandite (Figure 9b).

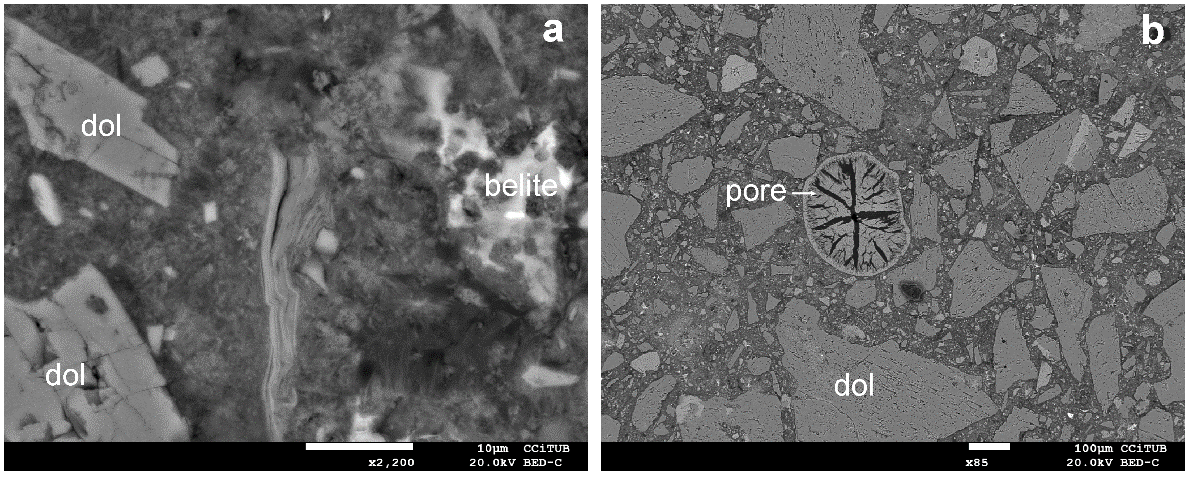

Figure 9. Backscattered-Scanning Electron Microscopy image of type B concrete. (**a**) Elongated illite crystal showing exfoliation planes, nodules of belite, and dolomite particles showing rhombohedral exfoliation imbibed in the cement paste; (**b**) regular distribution of dolomite particle of aggregate and fibrous crystals of ettringite filling a pore imbibed in the cement paste.

4. Discussion

The absence of brucite in the dolomitic rocks and its occurrence in the two types of concrete indicates that the dedolomitization reaction took place in the concrete from the Camarasa Dam. In the type A concrete, the reaction occurred on the surface of the dolomite aggregates, whereas in the type B concrete, the reaction mainly took place in the sand-cement paste and in the dolomite grain borders, although Blanco et al. [29] attributed a geological origin to the occurrence of brucite in the Camarasa Dam concrete.

In the reaction of dedolomitization, two processes are involved: the dissolution of dolomite and portlandite and the precipitation of new phases of brucite and calcite. The reaction of dedolomitization

proceeds until the consumption of portlandite [15]. The dissolution rate of dolomite depends on the mineral surface, which, in turn, depends on the particle sizes, and controls the kinetics of the reaction [14,20]. The most reactive dolomite aggregate was the finest fraction, <0.13 mm in the concrete of the Camarasa Dam. The two types of concrete exhibited differences in the content of this fraction of dolomite aggregates. In the type B concrete, all of the dolomite particles of this fraction were constituents of the sand-cement and were dispersed in the Portland cement.

In the type A concrete, the occurrence of portlandite in the paste indicates that this reaction can still take place. The Mg^{2+} removed from dolomite was accomplished with the OH^- from portlandite, and brucite precipitates as a rim around the partially dissolved dolomite grains (Figure 10).

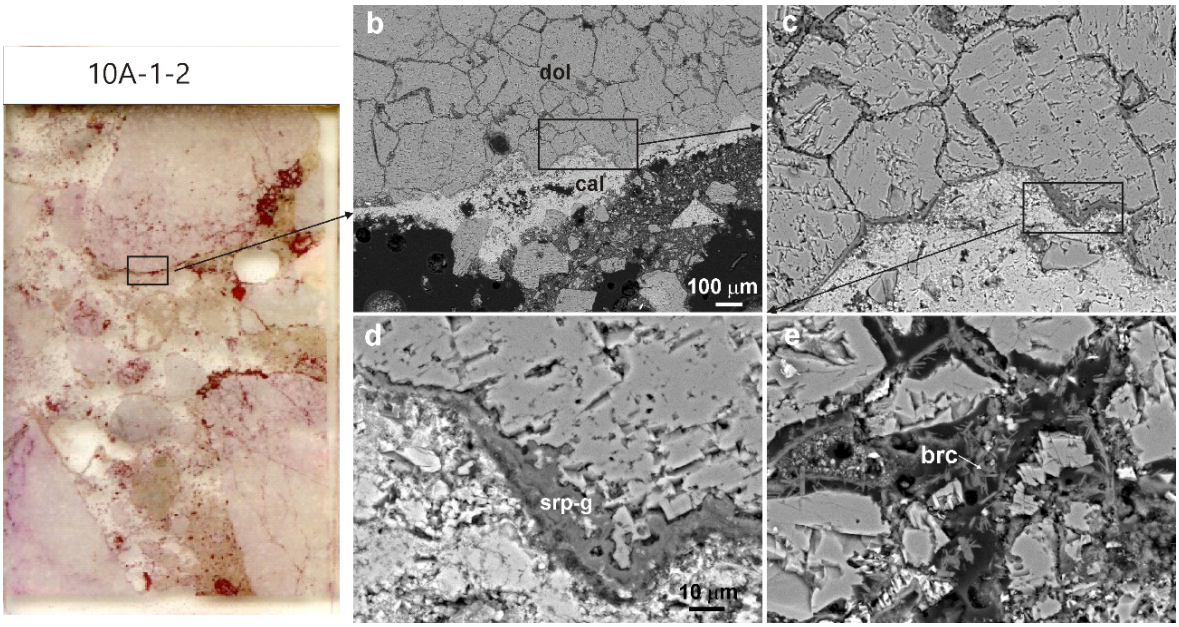

Figure 10. (**a**) Image of a thin section of the type B concrete stained with red alizarin; (**b**) SEM images of type B concrete that show the development of calcite and a rim of a serpentine group mineral; (**c**,**d**) details of this rim; (**e**) development of brucite in the sand-cement paste.

In addition to the precipitation of brucite, the dissolution of the Si, Al-rich phases of the cement paste removes the aluminum and silicon that substitute the Mg^{2+} from brucite. In this case, in order to balance the electrical charges, a coupled substitution of OH^- by CO_3^{2-} and a Mg rich rim is formed [30,31]. This rim constitutes a barrier that makes the dissolution of the dolomite aggregates difficult, as a result, the reaction of dedolomitization slows down [14,32,33].

In the reaction of dedolomitization, calcite is formed from the CO_3^{2-} and one Ca^{2+} provided by the dissolution of dolomite, and another Ca^{2+} provided by portlandite located in the cement paste. Then, most calcite is formed, not in direct contact with the dolomite aggregate, but in the contact point between the brucite rim and cement paste. A similar distribution of the products of the reaction of dedolomitization was obtained in experiments performed with a dolomite crystal immersed in an alkaline portlandite-rich solution [14]. In that case, brucite precipitated attached to the dolomite surface while most calcite precipitated in the solution.

In the type B concrete, the reaction of dedolomitization took place early, due to the high reactive surface of dolomite particles in the sand-cement paste. In this concrete, portlandite is dissolved and the OH^- anions are quickly trapped by the Mg^{2+} provided by dolomite in the sand-cement paste. Thus, brucite precipitates as fibrous crystals distributed in the sand-cement paste. The reaction consumes all available portlandite, and then, the coarser particles of dolomite aggregate will not be affected by the dedolomitization reaction. This process was also suggested for the dedolomitization reaction in batch experiments of dolomite dispersion in alkaline media [14].

Although the dedolomitization reaction occurred in both types of concretes, the visual inspection showed slight differences between types A and B, where A looked more compact than type B. The matrix of type B appeared more disaggregated and more fragile. However, the dedolomitization reaction was more extended in the conventional, or type A aggregate, as demonstrated by the higher proportion of calcite and brucite, which in turn decreased the binding properties and alkalinity of the matrix. The compression resistance of the cores from Camarasa confirmed these observations. Cabrera Vélez [34] reported mean values of 279.3 kg/cm^2 for the concrete of Portland cement and from 148.5 to 220.1 kg/cm^2 for concrete made with sand-cement. The parent density of both types of concrete [29] also showed that the alteration in the area that constituted of sand-cement was higher. Brucite has been considered as one of the main factors responsible for the loss of concrete durability [35]. However, in other cases, the highest expansion and loss of durability was attributed to the alkali-silica reaction (ASR) produced by the reactions due to the presence of quartz in the concrete matrix, which can accompany the dolomitic aggregates [36,37].

It can be considered that the concrete of the dam contains an excess of dolomite, whereas the amount of Portland cement, on the other hand, is significantly lower and therefore a limited amount of portlandite and silica gel will be produced. The pore solution in contact with these phases is subsatured in dolomite and CHS, which are thermodynamically unstable in this medium and will be dissolved. The dissolution of these phases produces two basic processes: (1) a dedolomitization reaction, which produces secondary calcite and brucite, and (2) between dolomite and the cement paste, a calcium silicate gel (CHS) gel is present, which reacts with brucite to produce a Mg-silicate gel that crystallizes in a serpentine group mineral. The formation of this mineral phase has also been reported in other concretes of dolomite aggregates [7,36,38].

$$\underset{\text{CSH}}{H_6Ca_3Si_2O_{10}} + \underset{\text{brucite}}{3Mg(OH)_2} = \underset{\text{serpentine group mineral}}{Mg_3(Si_2O_5)(OH)_4} + \underset{\text{portlandite}}{Ca(OH)_2} + H_2O \quad (2)$$

The kinetics of the dedolomitization reaction is controlled by the dissolution of the dolomite and the amount of portlandite available in the system. The reaction occurs very quickly for the smallest particles. For this reason, the mineralogical evolution of the system is qualitatively and quantitatively different in each of the concretes used for the construction of the dam.

The use of a concrete made with sand-cement contributes to the system with a particle size fraction of dolomite with an enormous reactive surface that confers to the reaction of dedolomitization a very fast kinetics. This reaction is completed in the sand-cement matrix by replacing the sand-cement paste in the surface, formed by dolomite and portlandite, with a mixture constituted of calcite and brucite. The agglomerating properties of brucite are not good enough and therefore the properties of the mechanical strength of the concrete are slightly diminished, as confirmed by the resistance behavior of the concrete made with sand-cement. Once the dolomite of the paste is consumed, a small fraction of portlandite remains undissolved and is susceptible to react with the larger grain size fractions of particles in the aggregate.

In the case of Portland concrete, the proportion of dolomitic aggregates with a reactive surface equivalent to that of the sand-cement dolomite particles was significantly lower. It was observed that the dedolomitization was produced by forming a reaction rim of less than 25 μm in thickness around the dolomite particles, consisting mainly of brucite, calcite, and a gel phase, and that a significant proportion of portlandite remained in the matrix of the concrete. The formation of a reaction rim around the aggregate hinders the dissolution of the dolomite, therefore the reaction occurs very slowly.

The gel phase is unstable in the system and evolves in the presence of Mg, forming hydrotalcite and serpentine group mineral, which are more stable in the system. Reaction (2) describes how the gel reacts with brucite, which is the product of the dedolomitization reaction, to form serpentine group mineral. Studies carried out on concretes attacked by magnesium sulfates show that serpentine group minerals have a low binder capacity with an appearance similar to that of the final stages of

concrete deterioration [30]. In the case of the Camarasa concrete, the magnesium source comes from the dissolution of dolomite and the presence of magnesium sulfate is not necessary.

Concrete constituted initially of dolomite and gel of the Portland cement in the appropriate ratios will evolve until reaching the equilibrium state with the formation of calcite and serpentine group mineral. The concrete of the Camarasa Dam has a large excess of dolomite that will not react. Given the reduced agglomerating properties of the serpentine group mineral, its difficulty of formation is rather beneficial, since it allows the gel life of the Portland to be extended. On the other hand, the formation of reaction rims on the surface of the dolomite is also an important factor in delaying the reactions that will produce the degradation of the concrete [39].

5. Conclusions

The concrete of the Camarasa Dam is made of aggregates mainly composed of dolomite. According to the dose, two type of concrete are distinguished: type A (dolomite and Portland cement) and type B (dolomite and sand-cement). The ACR occurs in both concrete types of the Camarasa Dam, forming calcite and brucite from the dissolution of dolomite in an alkaline media. In type A concrete, the dedolomitization reaction takes place on the surface of the aggregate particles and stops early, preserving the portlandite of the cement paste. In contrast, in the type B concrete, the reaction occurred in the sand-cement paste and all portlandite available was consumed very early by the dedolomitization reaction.

Although the brucite content was higher in type A concrete, type B showed more signs of loss of durability. This can be attributed to the greater development of the ASR in this concrete type.

In order to prevent the ACR, it is proposed that fractions smaller than 1 mm of the dolomite aggregate in the concrete are avoided completely.

Author Contributions: P.A. and E.T. wrote the paper; E.G. did the analytical work. All authors contributed to data interpretation and discussion. All authors have read and agreed to the published version of the manuscript.

Funding: This research was sponsored by the CICYT Spanish research project MAT2002-3345 and contract RED99-57. We thank ENDESA for providing the samples. The research was supported by the SGR-198 and SGR-707 of the Generalitat de Catalunya.

Acknowledgments: The SEM and electron microprobe analyses were performed at the Serveis Científico-Tècnics (SCT) de la Universitat de Barcelona with the assistance of R. Fontarnau, A. Domingo, and X Llovet. X-ray diffraction analyses were performed at the X-ray unit at the SCT (X. Alcobé). E. Garcia acknowledges the receipt of a FPU fellowship from the Spanish Ministerio de Educación y Cultura.

Conflicts of Interest: The authors declare no conflicts of interest.

References

1. Swenson, E.G. A Reactive Aggregate Undetected by ASTM Tests. *ASTM Bull.* **1957**, *226*, 48–51.
2. Swenson, E.G.; Gillott, J.E. Characteristics of Kingston carbonate rock reaction. *Highw. Res. Board Bull.* **1960**, *275*, 18–31.
3. Hadley, D.W. Alkali Reactivity of Carbonate Rocks-Expansion and Dedolomitization. *Highw. Res. Board Proc.* **1961**, *40*, 462–474.
4. Deng, M.; Tang, M.S. Mechanism of dedolomitization and expansion of dolomitic rocks. *Cem. Concr. Res.* **1993**, *23*, 1397–1408.
5. Tong, L.; Deng, M.; Lan, X.H.; Tang, M.S. A case study of two airport runways affected by alkali-carbonate reaction. Part one: Evidence of deterioration and evaluation of aggregates. *Cem. Concr. Res.* **1997**, *27*, 321–328. [CrossRef]
6. Gao, P.; Lu, X.; Geng, F.; Li, X.; Hou, J.; Lin, H.; Shi, N. Production of MgO-type expansive agent in dam concrete by use of industrial by-products. *Build. Environ.* **2008**, *43*, 453–457. [CrossRef]
7. Prinčič, T.; Štukovnik, P.; Pejovnik, S.; De Schutter, G.; Bosiljkov, V.B. Observations on dedolomitization of carbonate concrete aggregates, implications for ACR and expansion. *Cem. Concr. Res.* **2013**, *54*, 151–160. [CrossRef]

8. Tong, L.; Tang, M. Correlation between reaction and expansion of alkali-carbonate reaction. *Cem. Concr. Res.* **1995**, *25*, 470–476. [CrossRef]
9. Swenson, E.G.; Gillott, J.E. Alkali reactivity of dolomitic limestone aggregate. *Mag. Concr. Res.* **1967**, *19*, 95–104. [CrossRef]
10. Katayama, T. A critical review of carbonate rock reactions—Is their reactivity useful or harmful? In Proceedings of the 9th Int. Conf. on Alkali-Aggregate Reaction in Concrete (ICAAR), London, UK, 27–31 July 1992; pp. 508–517.
11. Charlwood, R.; Sims, I.A. Review of the Effectiveness of Strategies to Manage Expansive Chemical Reactions in Dams and Hydro Projects. In Proceedings of the Dam Swelling Concrete DSC, London, UK, 15 June 2017; p. 3.
12. Newell, V.A.; Wagner, C.D. Modifications to Hiwassee Dam and planned modification to Fontana and Chickamauga Dams by the Tennessee Valley Authority to manage alkali-aggregate reaction. In Proceedings of the 2nd Int. Conf. on Alkali-Aggregate Reaction in Hydroelectric Plants and Dams. USCOLD, Chattanooga, TN, USA, 22–27 October 1995; pp. 83–100.
13. Galí, S.; Ayora, C.; Alfonso, P.; Tauler, E.; Labrador, M. Kinetics of dolomite-portlandite reaction, Application to Portland cement concrete. *Cem. Concr. Res.* **2001**, *31*, 933–939. [CrossRef]
14. García, E.; Alfonso, P.; Labrador, M.; Galí, S. Dedolomitization in different alkaline media: Application to Portland cement paste. *Cem. Concr. Res.* **2003**, *33*, 1443–1448. [CrossRef]
15. García, E.; Alfonso, P.; Tauler, E.; Galí, S. Surface alteration of dolomite in dedolomitization reaction in alkaline media. *Cem. Concr. Res.* **2003**, *33*, 1449–1456. [CrossRef]
16. Wang, H.; Gillott, J.E. Alkali–carbonate reaction: significance of chemical and mineral admixtures. *Mag. Concr. Res.* **1995**, *47*, 69–75. [CrossRef]
17. Katayama. The so-called alkali-carbonate reaction (ACR)—Its mineralogical and geochemical details, with special reference to ASR. *Cem. Concr. Res.* **2010**, *40*, 643–675. [CrossRef]
18. Sant John, D.A.; Poole, A.W.; Sims, I. *Concrete Petrography*; Edward Arnold: London, UK, 1998; 474p.
19. Qian, G.; Deng, M.; Lan, X.; Xu, Z.; Tang, M. Alkali carbonate reaction expansion of dolomitic limestone aggregates with porphyrotopic texture. *Eng. Geol.* **2002**, *63*, 17–29. [CrossRef]
20. López-Buendía, A.M.; Climent, V.; Verdú, P. Lithological influence of aggregate in the alkali-carbonate reaction. *Cem. Concr. Res.* **2006**, *36*, 1490–1500. [CrossRef]
21. Girard, J.P.; Sanjuan, B.; Czernichowski-Lauriol, I.; Fouillac, C. Diagenesis of the Oseberg Sandstone Reservoir (North Sea): An example of integration of core, formation fluid and geochemical modelling studies. *AAPG Bull.* **1996**, *5*. (CONF-960527).
22. Lanza, V.; Alaejos, P. Optimized Gel Pat Test for Detection of Alkali-Reactive Aggregates. *ACI Mater. J.* **2012**, *109*, 403.
23. Lindgård, J.; Nixon, P.J.; Borchers, I.; Schouenborg, B.; Wigum, B.J.; Haugen, M.; Åkesson, U. The EU "PARTNER" Project—European standard tests to prevent alkali reactions in aggregates: Final results and recommendations. *Cem. Concr. Res.* **2010**, *40*, 611–635. [CrossRef]
24. Díez-Cascón, J.; Bueno, F. *Ingeniería de Presas: Presas de fábrica*; Univ. de Cantabria Publ. Santander: Cantabria, Spain, 2001; p. 474.
25. Solana, J. Sand-cement. *Rev. de Obras Públicas* **1916**, *64*, 85–88.
26. Martínez-Roig, J.M. *Instalación de la confluencia. Construcción de la presa de Camarasa, Col. Tècnico-Històrica de FECSA*; FECSA: Barcelona, Spain, 1995; 84p.
27. Pocoví, A. Estudio geológico de las Sierras Marginales Catalanas (Prepirineo de Lérida). *Acta Geol. Hisp.* **1998**, *XIII*, 73–79.
28. Rodríguez-Carvajal, J. An introduction to the program FullProf 2000, Laboratoire Leon Brillouin (CEA-CNRS), Gif-sur-Yvette, France. 2001. Available online: https://www.psi.ch/sites/default/files/import/sinq/dmc/ManualsEN/fullprof.pdf (accessed on 20 December 2019).
29. Blanco, A.; Segura, I.; Cavalaro, S.H.P.; Chinchón-Payá, S.; Aguado, A. Sand-cement concrete in the century-old Camarasa dam. *J. Perform. Constr. Facil.* **2015**, *30*. [CrossRef]
30. Hewlett, P.C.; Liska, M. *Lea's Chemistry of Cement and Concrete*; Butterworth-Heinemann: Oxford, UK, 2019.
31. Katayama, T.; Jensen, V.; Rogers, C.A. The enigma of the 'so-called'alkali–carbonate reaction. *Proc. Inst. Civ. Eng. -Constr. Mater.* **2016**, *169*, 223–232. [CrossRef]

32. Jin, F.; Wang, F.; Al-Tabbaa, A. Three-year performance of in-situ solidified/stabilised soil using novel MgO-bearing binders. *Chemosphere* **2016**, *144*, 681–688. [CrossRef]
33. Machner, A.; Zajac, M.; Haha, M.B.; Kjellsen, K.O.; Geiker, M.R.; De Weerdt, K. Stability of the hydrate phase assemblage in Portland composite cements containing dolomite and metakaolin after leaching, carbonation, and chloride exposure. *Cem. Concr. Res.* **2018**, *89*, 89–106. [CrossRef]
34. Cabrera Vélez, P.J. La Evolución de los Conglomerantes Hidráulicos en Presas. Master's Thesis, Universitat Politécnica de Catalunya, Barcelona, Spain, 2013.
35. Lee, H.; Cody, R.D.; Cody, A.M.; Spry, P.G. Observations on brucite formation and the role of brucite in Iowa highway concrete deterioration. *Environ. Eng. Geosci.* **2002**, *8*, 137–145. [CrossRef]
36. Katayama, T. How to identify carbonate rock reactions in concrete. *Mater. Charact.* **2004**, *53*, 85–104. [CrossRef]
37. Beyene, M.; Snyder, A.; Lee, R.J.; Blaszkiewicz, M. Alkali Silica Reaction (ASR) as a root cause of distress in a concrete made from Alkali Carbonate Reaction (ACR) potentially susceptible aggregates. *Cem. Concr. Res.* **2013**, *51*, 85–95. [CrossRef]
38. Locati, F.; Falcone, D.; Marfil, S. Dedolomitization and alkali-silica reactions in low-expansive marbles from the province of Córdoba, Argentina. A microstructural and chemical study. *Constr. Build. Mater.* **2014**, *58*, 171–181. [CrossRef]
39. Štukovnik, P.; Prinčič, T.; Pejovnik, R.S.; Bokan, B.V. Alkali-carbonate reaction in concrete and its implications for a high rate of long-term compressive strength increase. *Const. Building Mater.* **2014**, *50*, 699–709. [CrossRef]